

REPORT DOCUMENTATION PAGE		READ INSTRUCTIONS BEFORE COMPLETING FORM
1. REPORT NUMBER TR-275	2. GOVT ACCESSION NO.	3. RECIPIENT'S CATALOG NUMBER
4. TITLE (and Subtitle) Gulf Stream Surface Front Displacement by the Local Wind Stress: A Two-Dimensional Numerical Model		5. TYPE OF REPORT & PERIOD COVERED Technical Report
		6. PERFORMING ORG. REPORT NUMBER
7. AUTHOR(s) Charles W. Horton		8. CONTRACT OR GRANT NUMBER(s)
9. PERFORMING ORGANIZATION NAME AND ADDRESS Naval Oceanographic Office (Code 9110) NSTL Station Bay St. Louis, MS 39522		10. PROGRAM ELEMENT, PROJECT, TASK AREA & WORK UNIT NUMBERS
11. CONTROLLING OFFICE NAME AND ADDRESS		12. REPORT DATE April 1983
		13. NUMBER OF PAGES
14. MONITORING AGENCY NAME & ADDRESS (if different from Controlling Office)		15. SECURITY CLASS. (of this report) UNCLASSIFIED
		15a. DECLASSIFICATION/DOWNGRADING SCHEDULE
16. DISTRIBUTION STATEMENT (of this Report) Approved for public release; distribution unlimited.		
17. DISTRIBUTION STATEMENT (of the abstract entered in Block 20, if different from Report)		
18. SUPPLEMENTARY NOTES		
19. KEY WORDS (Continue on reverse side if necessary and identify by block number)		
20. ABSTRACT (Continue on reverse side if necessary and identify by block number) The displacement of the surface front of the Gulf Stream due to normally short but intense wind events such as hurricanes is modelled. The model is a relatively simple extension of a one-dimensional bulk mixed-layer model to two dimensions to allow the representation of the cross section of the mixed layer in the frontal zone of a strong current such as the Gulf Stream. The wind event is assumed to be a rapidly moving (11 m/s) circularly symmetric cyclone. Three different storm paths are modelled. All generate net shifts		

of the surface front relative to the subsurface front with inertial oscillations superimposed. One path is designed to simulate the passage of Hurricane Dennis during a Gulf Stream survey (Horton 1982). The net shift of the surface front predicted by the model compares reasonably with that observed.

LIBRARY
RESEARCH REPORTS DIVISION
NAVAL POSTGRADUATE SCHOOL
MONTEREY, CALIFORNIA 93943

TECHNICAL REPORT

GULF STREAM SURFACE FRONT DISPLACEMENT BY THE LOCAL WIND STRESS: A TWO-DIMENSIONAL NUMERICAL MODEL

CHARLES W. HORTON

APRIL 1983

APPROVED FOR PUBLIC RELEASE;
DISTRIBUTION UNLIMITED.

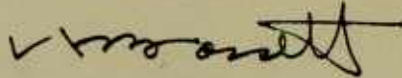
PREPARED BY
COMMANDING OFFICER,
NAVAL OCEANOGRAPHIC OFFICE ,
NSTL STATION, BAY ST. LOUIS, MS 39522

PREPARED FOR
COMMANDER,
NAVAL OCEANOGRAPHY COMMAND
NSTL STATION, BAY ST. LOUIS, MS 39529



FOREWORD

This Technical Report was prepared as part of a continuing effort to produce tactically useful products from satellite data by relating sea surface signatures to sub-surface thermal/acoustic structure. It was jointly funded by the Naval Oceanographic Office and the Naval Ocean Research and Development Activity under Satellite Oceanography Tactical Applications Program element 63704.

A handwritten signature in black ink, appearing to read 'C. H. Bassett', with a stylized flourish at the end.

C. H. BASSETT
Captain, USN
Commanding Officer

ACKNOWLEDGEMENTS

I wish to thank Edward Khedouri, Al Lewando and Mitch Shank for providing administrative and technical support for this project. I am grateful to Bob Coulter, John Bruce, John Blaha, and Alex Warn-Varnes for their critical comments during the manuscript review process.

CONTENTS

	<u>Page</u>
I. INTRODUCTION.....	1
A. Model Background.....	1
II. MODEL DEVELOPMENT.....	3
A. Mixed Layer Density Balance.....	3
B. Entrainment Model.....	3
C. Mixed Layer Continuity.....	4
D. Jump Condition for Density.....	4
E. Momentum Balance.....	5
III. SIMULATING HURRICANE PASSAGE.....	7
IV. RESULTS.....	8
A. Storm Path One.....	9
B. Storm Path Two.....	10
C. Storm Path Three.....	11
V. CONCLUSIONS.....	11
REFERENCES.....	13

FIGURES

Figure 1. Initial state of the model.....	15
Figure 2. Storm paths.....	16
Figure 3. Wind stress vectors as a function of time for the different storm paths.....	17
Figure 4. Cross stream displacement of the initial surface front due to the different storm paths.....	18
Figure 5a. Mixed layer density and depth changes due to storm path 1. Assumes confluence for the continuity balance and momentum balance A.....	19
Figure 5b. Mixed layer density and depth changes due to storm path 1. Assumes confluence for the continuity balance and momentum balance B.....	20
Figure 5c. Mixed layer density and depth changes due to storm path 1. Assumes convergence for the continuity balance and momentum balance A.....	21
Figure 5d. Same as figure 6c except that the cross stream velocity shear in the subsurface front is much weaker.....	22
Figure 6a. Mixed layer density and depth changes due to storm path 2. Assumes confluence for the continuity balance and momentum balance A.....	23
Figure 6b. Mixed layer density and depth changes due to storm path 2. Assumes confluence for the continuity balance and momentum balance B.....	24

Page

Figure 6c.	Mixed layer density and depth changes due to storm path 2. Assumes convergence for the continuity balance and momentum balance A.....	25
Figure 7a.	Mixed layer density and depth changes due to storm path 3. Assumes confluence for the continuity balance and momentum balance A.....	26
Figure 7b.	Mixed layer density and depth changes due to storm path 3. Assumes confluence for the continuity balance and momentum balance B.....	27
Figure 7c.	Mixed layer density and depth changes due to storm path 3. Assumes convergence for the continuity balance and momentum balance A.....	28

I. INTRODUCTION

Observational studies of the Gulf Stream front have shown the horizontal separation between the Gulf Stream surface and subsurface (15° isotherm at 200m) fronts to be quite variable. Early studies such as those by Hansen and Maul (1975) and Khedouri, et al. (1976) had insufficient wind data to definitely correlate changes in separation with the passage of storms, although Hansen and Maul did suggest that there was a relationship.

During August 1981 the Naval Oceanographic Office (NAVOCEANO) conducted a survey of the Gulf Stream northeast of Cape Hatteras to study the relationship between the paths of the Gulf Stream's surface and subsurface fronts and the local wind stress (Horton, 1982). During this experiment the center of Hurricane Dennis passed from west to east approximately 30km to 100km south of the portion of the Gulf Stream under observation. At the same time the average separation between the surface and subsurface fronts increased from about 1km to about 19km. Since the zonal component of the winds was from the east during the passage of Dennis, the increase in separation is consistent with a displacement of the surface front to the right of the wind by advection in the mixed layer.

In this study we model and predict the displacement of the surface front of the Gulf Stream due to short but intense wind events and compare the results of this effort to the observed displacement of the surface front by Hurricane Dennis. The model is a relatively simple extension of a one-dimensional bulk mixed-layer model to two dimensions to permit the representation of a cross section of the mixed layer in the frontal zone of a strong current. No downstream variations of the front are allowed. A secondary purpose is to illustrate how strong mixing or cross stream mass convergences might lead to the formation of new surface fronts or the destruction of existing ones.

A. Model Background.

Earlier efforts by de Szoeke (1980) and Cushman-Roisin (1981) have extended one dimensional mixed layer models to two dimensions, but their efforts differ substantially from this one in that their initial states do not contain fronts. These models start with meridional temperature gradients characteristic of the open ocean. They are primarily interested in the formation of horizontal variation (especially fronts) in the surface temperature field on the seasonal time scale, although the de Szoeke model is also valid during the first inertial day.

According to Cushman-Roisin (1981) there are two major classes of mixed layer models: a) turbulent erosion models (TEM), and b) dynamic instability models (DIM). In order to describe the differences between them, we write the simplified potential energy (PE) budget for the mixed layer as

$$\frac{dPE}{dt} = F_S - D + E . \quad (1)$$

$F_S - D$ is the surface flux due to wave breaking minus internal dissipation in the mixed layer. E is the rate of production due to the mean shear at the base of the mixed layer. TEM models neglect E and attribute the time rate of

change of the potential energy to the surface flux minus internal dissipation. DIM models do the opposite and consider only the change in potential energy due to mean shear at the base of the mixed layer.

De Szoeke and Rhines (1976) state that a DIM is appropriate for the first inertial period after the onset of a wind stress forcing a fluid initially at rest. For longer times a TEM is appropriate. Klein and Coantic (1981) modeled the mixed layer using a second-order turbulence closure model. They concluded that the significance of turbulent kinetic energy input due to surface wave breaking is limited to the first few meters of depth, and that when the depth is greater than this, the mixed-layer deepening is driven primarily by the shear instability at the base of the mixed layer. This conclusion supports the observations of mixed-layer deepening by Price, *et al.* (1978) who found that the deepening is highly intermittent on the storm time scale and that it is the velocity shear at the base of the mixed layer and not the magnitude of the local wind stress which is the most relevant controlling factor.

Because of the short time scale involved related to a storm passage, it is clear that a DIM should be used. A TEM could only be valid over a seasonal cycle, although its validity even on this time scale is not certain because mixed-layer deepening can be highly intermittent and largely confined to storm passages.

The first slab model of the mixed layer using the DIM mechanism was by Pollard, *et al.*, (1972). It is based upon the assumption that the mixed layer will remain marginally dynamically unstable. This assumption is manifested by requiring that the bulk Richardson number

$$Ri = \frac{g\Delta\rho h}{\rho(u^2+v^2)} \quad (2)$$

always have the value unity. Here h is the mixed layer depth and $\Delta\rho$, u , and v are the density and velocity jumps at the base of the mixed layer.

As an alternative to requiring that Ri remain equal to one, Phillips (1977) postulated that the rate of deepening due to entrainment is

$$\frac{\partial h}{\partial t} = (u^2 + v^2) F(Ri) \quad (3)$$

where F is an unknown function of Ri . Price (1979) determined F using experimental measurements of mixed layer deepening. His parametrization of entrainment is used to predict mixed layer deepening.

In this model the surface front moves via cross stream advection in the mixed layer. To illustrate this, consider initially the case where density is conserved in the mixed layer. Continuity of density is expressed as

$$\frac{d\rho}{dt} = \frac{\partial\rho}{\partial t} + v\frac{\partial\rho}{\partial y} = 0. \quad (4)$$

Here v is the cross stream (northward) velocity and y is the cross stream (northward) coordinate. Equation (4) can be rearranged to the form

$$\left(\frac{\partial y}{\partial t}\right)_\rho = v. \quad (5)$$

This form of (4) shows that the cross stream speed holding density constant is v . Because we assumed no mixing, the surface front (or any surface feature identifiable by its density) moves with speed v .

However, in general, density in the mixed layer is not conserved due to entrainment of cooler, deeper layer water at the base of the mixed layer. The determination of the density balance in the mixed layer and the speed at which the surface front is advected requires that this entrainment be described.

II. MODEL DEVELOPMENT

Our model consists of a mixed layer with a narrow density front overlying a lower layer with a density front. Figure 1 illustrates the initial state of this model before the start of the wind stress forcing. We start with the surface front overlying the subsurface front. The density field varies slowly on each side of the surface and subsurface fronts. In the lower layer the downstream velocity U_0 and the Brunt-Vaisiala frequency N are prescribed. They vary with cross stream position but are not allowed to change with time. The lower layer can be vertically "pumped" when convergence occurs in the mixed layer. At the base of the mixed layer there are the density and velocity jumps $\Delta\rho$, u , and v . Initially u and v are zero. The density jump $\Delta\rho$ and the mixed layer depth h are given initial values.

A. Mixed Layer Density Balance

When entrainment occurs,

$$\frac{d\rho}{dt} = \frac{\partial\rho}{\partial t} + \frac{v\partial\rho}{\partial y} = \frac{\partial h_e}{\partial t} \frac{\Delta\rho}{h} \quad (6)$$

where h_e is the increase in mixed layer depth due to entrainment. There can also be a flux of density from the atmosphere to the mixed layer, but this effect is not considered. Price (1981), in modelling the response of the upper ocean to a moving hurricane, found that air-sea heat exchange plays only a minor role relative to entrainment in changing the mixed layer density.

B. Entrainment Model

In order to predict the rate of mixed layer deepening due to entrainment, we use a DIM (model) by Price (1979). Using the experimental results on stress-driven entrainment of Kato and Philips (1969) and Kanthe, et al. (1978), Price determined that

$$\frac{\partial h_e / \partial t}{(u^2 + v^2)^{1/2}} = \begin{cases} 5 \times 10^{-4} Ri^{-4} & \text{if } Ri \leq 1 \\ 0 & \text{if } Ri > 1 \end{cases} \quad (7)$$

C. Mixed Layer Continuity

The equation of continuity integrated over the depth of the mixed layer is

$$h \frac{\partial u}{\partial x} + h \frac{\partial v}{\partial y} - w_b = 0. \quad (8)$$

Here w_b is the vertical velocity (following a parcel) at the base of the mixed layer. It is assumed that the vertical velocity at the surface is zero.

We define h_c to be the change in depth of the mixed layer due to a cross stream convergence of mass in the mixed layer. Its sign is positive when the increase in depth is positive. Since

$$-w_b = \frac{\partial h_c}{\partial t} + v \frac{\partial h}{\partial y} + (U_0 + u) \frac{\partial h}{\partial x} \quad (9)$$

Equations (8) and (9) show that

$$\frac{\partial h_c}{\partial t} = - \frac{\partial(vh)}{\partial y} - \frac{\partial((U_0 + u)h)}{\partial x} \quad (10)$$

The cross stream convergence must be balanced, as (10) shows, by deepening of the mixed layer and/or by a downstream convergence. Since the model is only two-dimensional (2-D), it cannot tell how the cross stream convergence is partitioned. Therefore, we only consider the two limiting cases where

$$\frac{\partial h_c}{\partial t} = - \frac{\partial(vh)}{\partial y}; \quad \frac{\partial((U_0 + u)h)}{\partial x} = 0, \quad \text{or} \quad (11)$$

$$\frac{\partial h_c}{\partial t} = 0; \quad \frac{\partial((U_0 + u)h)}{\partial x} = - \frac{\partial(vh)}{\partial y}. \quad (12)$$

Using the same terminology as Cushman-Roisin (1982), we denote (11) to be **convergence** and (12) to be **confluence**.

The total deepening rate $\partial h / \partial t$ of the mixed layer is the sum of the deepening rates due to convergence and entrainment. For the case of **confluence**, $\partial h / \partial t$ is equal to $\partial h_e / \partial t$. For the case of **convergence**

$$\frac{\partial h}{\partial t} = \begin{cases} 5 \times 10^{-4} (u^2 + v^2)^{1/2} Ri^{-4} - \frac{\partial(vh)}{\partial y} & \text{if } Ri \leq 1 \\ - \frac{\partial(vh)}{\partial y} & \text{if } Ri > 1 \end{cases} \quad (13)$$

D. Jump Condition for Density

The density jump across the interface at the base of the mixed layer is

$$\Delta \rho = \rho_l - \rho \quad (14)$$

where ρ is the mixed layer density and ρ_ℓ is the density in the lower layer immediately below the base of the mixed layer. It is also the density of the water entrained into the mixed layer.

We define a ρ_{ℓ_0} as the initial ρ_ℓ . We also assume that the lower layer has constant stratification N . After the initiation of the wind stress, ρ_ℓ changes as the mixed layer deepens. Consider the case of **confluence** where the mixed layer deepens only due to entrainment. For this case

$$\Delta\rho = \rho_{\ell_0} + h_e \frac{\rho_0 N^2}{g} - \rho \quad (15)$$

where ρ_0 is a reference density chosen to be 1 gm/cm^3 for simplicity.

For the case of **convergence** it is also necessary to consider the pumping of the lower layer. The initial response of the lower layer to the pumping is solely the vertical displacement of lower layer water parcels. This simply moves the lid of the lower layer up or down leaving ρ_ℓ and hence the validity of (15) unchanged. Later as the pumping spins up the lower layer, horizontal advective terms will be induced there. The cross stream advection of density in the lower layer will alter ρ_ℓ and reduce the validity of (15). However, because we are modelling the mixed layer for about one day, we ignore this later response and assume that (15) remains valid for the case of **convergence** as well.

E. Momentum Balance

Integrated over the depth h of the mixed layer, the momentum balances are

$$\frac{\partial(uh)}{\partial t} - u \frac{\partial h_c}{\partial t} - \left(f - \frac{\partial U_0}{\partial y} - \frac{\partial u}{\partial y} \right) vh = \frac{\tau_x}{\rho} + D_x, \quad \text{and} \quad (16)$$

$$\frac{\partial(vh)}{\partial t} - v \frac{\partial h_c}{\partial t} + fuh = \frac{\tau_y}{\rho} + D_y - \frac{h}{\rho} \left(\frac{\partial P}{\partial y} - \frac{\partial P_0}{\partial y} \right). \quad (17)$$

where we have assumed

$$fU_0 = - \frac{1}{\rho} \frac{\partial P_0}{\partial y}, \quad (18)$$

$$\frac{\tau(z=-h)}{\rho} = u \frac{\partial h_e}{\partial t}, \quad \text{and} \quad (19)$$

$$\frac{\partial P}{\partial y} - \frac{\partial P_0}{\partial y} = - \frac{gh\partial\rho}{2\partial y} - \frac{g\Delta\rho}{\rho} \frac{\partial h}{\partial y}. \quad (20)$$

In (16) and (17) D_x and D_y are terms representing frictional damping. τ_x and τ_y are respectively the east and north components of the wind stress τ . Equation (19) used by Pollard, et al., (1972) says that the stress at the base of the mixed layer $\tau(z=-h)$ is used to bring the momentum of entrained lower layer water up to that of the mixed layer.

Outside the surface front the frictional damping terms are probably minor (especially relative to the wind stress τ which we assume to be large). Inside the very narrow surface front they may not be, but we do not know how to accurately represent them. Therefore, two different types of simplifying assumptions will be compared.

The first simplifying assumption attempted is to assume D_x and D_y to be everywhere negligible. Equations (16) and (17) become

$$\frac{\partial(uh)}{\partial t} - u \frac{\partial h_c}{\partial t} - \left(f - \frac{\partial U_0}{\partial y} - \frac{\partial u}{\partial y} \right) vh = \frac{\tau_x}{\rho} \quad , \quad \text{and} \quad (21)$$

$$\frac{\partial(vh)}{\partial t} - v \frac{\partial h_c}{\partial t} + fuh \approx \frac{\tau_y}{\rho} - \frac{h}{\rho} \left(\frac{\partial P}{\partial y} - \frac{\partial P_0}{\partial y} \right). \quad (22)$$

At the start of each run of the model before the advent of the wind stress, we assume that the mixed layer flow is in geostrophic balance, i.e.,

$$fu_i = \frac{gh_i}{2\rho} \frac{\partial \rho_i}{\partial y} \quad \text{and} \quad (23)$$

$$v_i = 0. \quad (24)$$

The i subscripts imply initial values. The mixed layer depth h_i is a constant ($\partial h_i / \partial y = 0$).

The alternative type of simplification of (16) and (17) stems from considering the momentum balances away from the surface front. Away from surface fronts $\partial P / \partial y - \partial P_0 / \partial y$ is a minor term since the mixed layer density and depth gradients are small. For the same reason u should be much less than U_0 so that $\partial u / \partial y$ can be neglected relative to $\partial U_0 / \partial y$ in (16). As before, the frictional damping terms are neglected as well. Hence, away from surface fronts (16) and (17) become

$$\frac{\partial(uh)}{\partial t} - u \frac{\partial h_c}{\partial t} - \left(f - \frac{\partial U_0}{\partial y} \right) vh = \tau_x \quad , \quad \text{and} \quad (25)$$

$$\frac{\partial(vh)}{\partial t} - v \frac{\partial h_c}{\partial t} + fuh = \tau_y. \quad (26)$$

The first type of simplification of (16) and (17) assumes that the pressure gradient $\partial P / \partial y - \partial P_0 / \partial y$ in the surface front is balanced by the inertial and Coriolis terms. However, since the surface front can be a kilometer or less in width, the momentum balance there is likely to be highly frictional. Therefore, the second type of simplification of (16) and (17) assumes that the surface front is in frictional balance, i.e.,

$$\frac{\partial P}{\partial y} - \frac{\partial P_0}{\partial y} = D_y \quad (27)$$

This assumption is very convenient because equation (26), the cross stream momentum balance, is now appropriate everywhere, not just away from surface fronts. Accordingly, u will not change suddenly from inside the surface front to outside it. Therefore it is consistent to assume $\partial u/\partial y$ to be minor relative to $\partial U_0/\partial y$ in the surface front as well and also assume (26) to be valid everywhere. Using (25) and (26) to describe the motion of the surface front makes sense if one thinks of the surface front as being an arbitrarily thin interface between two water masses of differing density. The interface moves simply with the speed of the water masses immediately on each side of it.

To summarize, two different simplifications of (16) and (17) given respectively by (21) and (22) and by (25) and (26) are tried. The major difference between the two is that the first type of simplification includes the pressure gradient term $\partial P/\partial y - \partial P_0/\partial y$ while the second does not. For later use we call the simpler momentum balance which excludes the pressure gradient term momentum balance A. The more complete momentum balance is called momentum balance B.

The model is solved numerically using a 100 meter cross stream resolution (grid scale) and a 100 second time step. Momentum balance B proved to be unstable. To counteract this, the solution was smoothed slightly after every time step with the intent of removing grid scale instabilities. This was done by averaging the solution in each grid with its two immediate neighbors using a normalized one-twelve-one running average. The model solutions assuming momentum balance A and **confluence** were obtained with and without smoothing. Except for slightly broader surface fronts, the smoothing made little essential difference. For better comparison with the solutions assuming B, all solutions assuming A displayed in the results are those that have been smoothed.

III. SIMULATING HURRICANE PASSAGE

In this model we vary the wind stress in direction and magnitude with time as well as with a cross stream position consistent with the passage of Hurricane Dennis. We compute the wind stress by assigning the storm's

- a. wind stress distribution,
- b. speed and direction, and
- c. initial position relative to the 2-D section of the surface front.

Because the size and strength of Dennis were only roughly known, for simplicity we assume the storm to be circularly symmetric and to have a Gaussian stress envelope. This envelope is specified by assigning the wind stress at the storm's center and at some radius from its center. This is analogous to the manner in which the strength of a hurricane is reported by giving the wind speed at its center and the radius of its gale force winds. The storm may have any starting point, speed, and direction, but the speed, course, and strength of the storm is held fixed during its passage. During the simulation of the storm's passage the direction and distance to the storm as a function of cross stream position are continuously computed. These

parameters, together with the assigned wind stress distribution of the storm, allow the wind stress direction and magnitude to be continuously determined.

Referring to figure 2 in Horton (1982), we see that Dennis traveled a path essentially parallel to that of the Gulf Stream on the average of about 40 km to 50 km to the south of the subsurface front. The figure also shows that during its passage Dennis decreased in maximum strength and was downgraded to a Tropical Storm. However, National Hurricane Center advisories show that as its maximum windspeeds decreased, its radius of gale force (34 knots) winds increased. Based upon these advisories we assume the wind speed at the storm's center to be 60 knots (30 m/s) and the radius of its gale force winds to be 200 nm (370 km). Wind stress is computed from wind speed using

$$\tau = \rho_a C_D U_{10}^2 \quad (28)$$

where ρ_a is air density, U_{10} is the wind speed at 10m above the sea surface, and C_D is the drag coefficient. Bunker (1976) summarized the drag coefficient calculations of many investigators. The experimental drag coefficients show much scatter and are evidently not known accurately. We assume Garrett's (1977) form for C_D ,

$$C_D = (0.73 + 0.069 U_{10}) \times 10^{-3} \quad (29)$$

Using this expression, C_D equals 2.8×10^{-3} when U_{10} is 30 m/s, and 1.9×10^{-3} when U_{10} is 17 m/s. The wind stress is estimated to be 30 dynes/cm² at the storm's center and to be 6 dynes/cm² at a radius of 370 km.

In order to simulate the hurricane's passage, it is assumed that the storm travels due east 44 km to the south of the initial position of the surface front at 11 m/s (40 km/hr). We also try two other storm paths to show in a more general manner how a hurricane can affect the Gulf Stream surface front.

IV. RESULTS

The three different storm paths used to model surface front advection are illustrated in figure 2. For each of these paths the storm travels at the same speed, 11 m/s, and has the same size and strength. Figure 3 shows the wind stress vectors as a function of time for these paths at the initial location of the surface front (the location of the subsurface front). In figure 4 the displacements of the initial surface front are shown as a function of time. This figure is computed assuming **confluence** for the continuity balance and the simpler momentum balance A. Essentially the same results are obtained if **convergence** for the continuity balance or the more complete momentum balance are used instead.

Finally, figures 5(a, b, c), 6(a, b, c), and 7(a, b, c) illustrate respectively for the three storm paths the mixed layer densities and mixed layer depths as a function of cross stream position at several times (0, 8, 15, and 22 hours). Figures 5a, 6a, and 7a assume **confluence** for the continuity balance and case A (where the pressure gradient $\partial P/\partial y - \partial P_0/\partial y$ is neglected) for the momentum balance. Figures 5b, 6b, and 7b also assume

confluence for the continuity balance but in conjunction with the more complete momentum balance B. Figures 5c, 6c, and 7c use the simpler momentum balance A but assume **convergence** for the mass balance. There is also a figure 5d which is identical to 5c except that the prescribed subsurface front in 6d is much weaker.

A. Storm Path One

The wind stress for this path is dominantly to the west as shown by figure 3. Figure 4 shows that the surface front is advected to the north (to the right of the wind) as expected. As for all of the storm paths, there is a strong inertial oscillation superimposed on the net displacement of the surface front. Figure 4 covers half an inertial cycle in which we see the surface front oscillating between 17.5 km and 8.5 km north of its initial position. We assume the average of these two values, 13 km, to be the net displacement of the surface front by the wind. This compares with a shift of 18 km observed due to the passage of Dennis (Horton, 1982).

Figures 5a, 5b, and 5c show the maximum and minimum shifts of the surface front at 15 and 22 hours respectively. While they all show similar shifts in the initial surface front, this similarity does not extend to mixed layer depth and density. Figures 5a and 5b which both assume **confluence** give similar mixed layer depths and densities. However, figure 5c which assumes **convergence** differs substantially in this regard.

Comparing the case assuming **convergence** with the cases assuming **confluence**, the mixed layer density and depth at 8 hours are very similar. At 15 hours, though, the **convergence** case shows strong changes in mixed layer depth and density arising from cross stream convergences of mass. From about 0 km to -10 km there is upwelling while from about -10 km to -20 km there is downwelling. The upwelling and downwelling are due to wind stress induced **convergences** of mass.

In order to understand why this occurred, consider equation (25) where the local time rate of change of u_h is neglected.

$$\left(f - \frac{\partial U_0}{\partial y}\right) v_h = -\tau_x \quad (30)$$

Rearranging this equation and combining it with (11) yields

$$\frac{\partial h_c}{\partial t} = \frac{\partial}{\partial y} \left(\frac{\tau_x}{f - \partial U_0 / \partial y} \right) \quad (31)$$

In the subsurface front $\partial U_0 / \partial y$ changes much more rapidly with cross stream position than τ_y . Thus

$$\frac{\partial h_c}{\partial t} \approx \frac{\tau_x}{(f - \partial U_0 / \partial y)^2} \frac{\partial^2 U_0}{\partial y^2} \quad (32)$$

Equation (32) tells us that a wind stress with no curl can induce intense Ekman pumping in a frontal zone. This effect was first described by Niiler (1969).

Figure 3 shows us that shortly before 15 hours τ_x was large and negative. Between 0 km and -10 km $\partial^2 U_0 / \partial y^2$ is positive while between -10 km and -20 km $\partial^2 U_0 / \partial y^2$ is negative. Therefore, equation (32) predicts upwelling (h decreases) between 0 km and -10 km and downwelling between -10 km and -20 km. This is exactly as figure 5c shows at 15 hours.

After 16 hours the mixed layer water parcels inertially oscillate with little wind driving. However, adjacent water parcels have different inertial amplitudes and frequencies largely because of cross stream changes in the effective Coriolis frequency $f - \partial U_0 / \partial y$. The different inertial frequencies force adjacent fluid parcels to have their respective inertial cycles become increasingly out of phase with time. The net result of the different inertial amplitudes and phases of adjacent fluid parcels is intense variability at the inertial frequency in mixed layer mass convergences and hence mixed layer depths.

At 22 hours the differences between figures 5b and 5c have become even more extreme. Figure 5c shows that by this time a dense region has formed to the south of the original surface front. The southern edge of this dense region is a new surface front. The dense region has formed because the large gradients in mixed layer depths due to assuming **convergence** have led to a large value of $v \partial \rho / \partial y$ there. The mixed layer depths at 22 hours in figure 5c are very chaotic. Since after 16 hours the zonal component of the local wind stress is weak, the chaotic mixed layer depths are not wind induced in the manner of (32). The mixed layer depth changes are similar, though, in that they are for the most part due to large cross stream changes in $\partial U_0 / \partial y$.

In order to verify this, another run of the model assuming **convergence** was made with the maximum $\partial U_0 / \partial y$ reduced from -.6 (as illustrated in figure 3) to -.1. The result, shown in figure 5d, is substantially equivalent to assuming **confluence**.

However, the results assuming **convergence** are at least superficially similar to observations of the Iceland-Faeroe Current by Von Zweck and Tieg (1982). They observed alternating warm and cool regions (and multiple fronts) across the current. In this area the horizontal temperature-salinity (TS) curves were the same as the vertical TS curves. This likeness is consistent with the alternating warm and cool regions and associated fronts being due to downwelling or upwelling.

B. Storm Path Two

The next storm path is also parallel to the stream, but is north of the subsurface front the same distance path one is to the south. This path yields, as figure 3 shows, meridional wind stresses the same as for the first storm path, but zonal wind stresses opposite in sign. As figure 4 shows, the surface front initially moves to the north, then to the south. The net southern displacement is expected because the zonal component of the wind stress is positive. Assuming **confluence** or **convergence** yields essentially identical surface front displacements.

As with the first storm path, the two cases assuming confluence are very similar. At 15 hours the original surface front is near 4 km and has weakened somewhat. Near -4 km a second wider surface has formed. It is due to entrainment of cooler, underlying water to the south of the subsurface front than to the north of the subsurface front.

Figure 4 shows that after 13 hours the original surface front is advected to the south. When the flow is to the south in the mixed layer, relatively dense mixed layer water is moved over suddenly less dense lower layer water. This leads to a much reduced bulk Ri number and greatly enhanced entrainment at the base of the mixed layer. Consequently at 22 hours we see a very deep mixed layer immediately to the south of the subsurface front.

At 22 hours figure 4 shows the northern edge of the original surface front to be near -18 km. It has become spread out and diffuse and merges into a broad decrease in mixed layer density south of the subsurface front. After 22 hours the original surface front loses its identity and becomes impossible to follow. Figure 6c which assumes **convergence** also shows the surface front becoming broad and diffuse at 22 hours. However, an exceedingly deep mixed layer in excess of 200 meters has formed over the subsurface front. As with the first storm path this is primarily due to sharp cross stream changes in $\partial U_0 / \partial y$ there.

C. Storm Path Three

For this final situation the storm path is purely meridional and to the east of the section of the modeled current. As figure 3 shows, this yields wind stresses whose meridional components are always negative. Because the winds have zonal symmetry during the storm's passage, one might expect the surface front to inertially shake about its original position. However, figure 4 shows that there is a net northward displacement of the surface front which occurs because the mixed layer depth increases with time. This deepening of the mixed layer dampens the movement of the surface front making the inertial oscillation nonsymmetric.

Overall, this storm path gives results very close to those of the first storm path. The major difference is that the surface front at 22 hours in figure 7a, the case which assumes **confluence** for the continuity balance and the more complete momentum balance, has lost its identity. The surface front in figure 7c at 22 hours has weakened substantially as well. Its remnant is seen at 5 km. Of interest is the very intense new surface front which formed to the south of the original one. Associated with this new surface front we again see large subsurface mixed layer depth changes due to cross stream convergences and divergences of mass.

V. CONCLUSIONS

Assuming **confluence** for the mixed layer continuity balance, two degrees of simplification of the mixed layer momentum balances were employed. The more complete momentum balance includes the cross stream pressure gradient due to cross stream changes in mixed layer density and depth while the simpler momentum balance does not. Including or disregarding this pressure gradient made little difference upon frontal displacement. The simpler momentum balance was also tried assuming **convergence**. Again the observed frontal

displacements remained essentially the same, although significant differences in the details of the mixed layer density structure and depth were observed. This observation is consistent with the results of Price (1981) who found that mixed layer velocities during a hurricane's passage are primarily sensitive to the wind stress.

The first storm path was intended to roughly simulate the passage of Hurricane Dennis during a Gulf Stream survey by Horton (1982). The model predicted a shift of the surface front relative to the subsurface front of about 13 km. This compares to an observed shift of about 18 km. Considering the crudeness of our knowledge of the wind stress during Dennis' passage, this agreement is quite reasonable. Also obscuring the difference between the observed and predicted shifts is the inertial oscillating of the predicted surface front displacement.

The details of the density structure in the mixed layer are very sensitive to whether **confluence** and **convergence** are assumed. As was shown, these greatly different results arise primarily from large cross stream changes in $\partial U_0/\partial y$ in the subsurface front. The changes in $\partial U_0/\partial y$ induce substantial cross stream convergences in mass flux. In the cases assuming **convergence** for their continuity balances, the mass convergences cause Ekman pumping. These cases give the impression of being too extreme and thus unrealistic. However, they strongly suggest that substantial variability in mixed layer depths at the inertial frequency should be expected in frontal regions.

The model also shows that the rate of mixed layer deepening due to entrainment is strongly dependent upon the sign of the cross stream advection in the mixed layer. Northward advection, as associated with the first storm path, results in relatively light mixed layer water moving over suddenly more dense lower layer water as it crosses over the lower layer front. A relatively large bulk Richardson number and a relatively low entrainment rate are a consequence. Southward advection, as occurring with the second storm path, results in mixed layer water moving over suddenly less dense lower layer water. As figures 6a and 6b show, a very deep mixed layer immediately to the south of the subsurface front is formed as a consequence of the low bulk Richardson number.

The primary purpose of the model is to predict the displacement of an existing surface front. The model is judged suitable for this purpose. Its most pragmatic version is the version using the simplest momentum balance and assuming **confluence**. The model, however, is not suitable for predicting the details of the mixed layer structure when a strong subsurface front is present. A two dimensional model simply cannot distinguish between the two limiting cases of **confluence** or **convergence** for the continuity balance. A three dimensional model may be necessary if the details of the mixed layer structure in a frontal zone are to be accurately predicted.

REFERENCES

- Bunker, A. F., Computations of surface energy flux and annual air-sea interaction cycles of the North Atlantic Ocean, Mon. Wea. Rev., 104, 1122-1140, 1976.
- Cushman-Roisin, B., Deepening of the wind-mixed layer: A model of the vertical structure, Tellus, 33, 544-582, 1981.
- de Szoeke, R. A., On the effects of horizontal variability of wind stress on the dynamics of the ocean mixed layer, J. Phys. Oceanogr., 10, 1439-1455, 1980.
- de Szoeke, R. A. and Rhines, P. B., Asymptotic regimes in mixed-layer deepening, J. Mar. Res., 34, 111-116, 1976.
- Garrett, J. R., Review of drag coefficients over oceans and continents, Mon. Wea. Rev., 105, 915-929, 1977.
- Hansen, D. V. and G. Maul, A note on the use of sea surface temperature for observing ocean currents, Remote Sensing of the Environment, 1, 161-164, 1970.
- Horton, C. W., Preliminary report on inferring the path of the subsurface front of the Gulf Stream from surface infrared observations, Technical Note TN 9100-9-81, Naval Oceanographic Office, NSTL Station, Bay St. Louis, MS, 1982.
- Kantha, L. H., O. M. Phillips, and R. S. Azad, On turbulent entrainment at a stable interface, J. Fluid Mech., 79, 753-768, 1977.
- Kato, H., and Phillips, O. M., On the penetration of a turbulent layer into a stratified fluid, J. Fluid Mech., 37, 643-665, 1969.
- Khedouri, E., W. Gemmil, and M. Shank, Statistical summary of ocean fronts and water masses in the western North Atlantic, Reference Publication 9, 24, Naval Oceanographic Office, NSTL Station, Bay St. Louis, MS, 1976.
- Klein, P. and M. Coantic, A numerical study of turbulent processes in the marine upper layers, J. Phys. Oceanogr., 11, 849-863, 1981.
- Niiler, P. P., On the Ekman divergence in an oceanic jet, J. Geophys. Res., 74, 7048-7052, 1969.
- Phillips, O. M., Entrainment, Chap. 7 in E. B. Krauss (Editor), Modelling and prediction of the upper layers in the ocean, Pergamon Press, 1977.
- Pollard, R. T., P. B. Rhines and R.O. R. Y. Thompson, The deepening of the wind-mixed layer, Geophys. Fluid Dyn., 4, 381-404, 1972.
- Price, J. F., On the scaling of stress driven entrainment experiments, J. Fluid. Mech., 90, 502-529, 1979.
- Price, J. F., Upper ocean response to a hurricane, J. Phys. Oceanogr., 11, 153-175, 1981.

Price, J. F., C. Mooers, and J. Van Leer, Observation and simulation of storm-induced mixed layer deepening, J. Phys. Oceanogr., 8, 582-599, 1978.

Von Zweck, O. and W. Teague, Private communication, 1982.

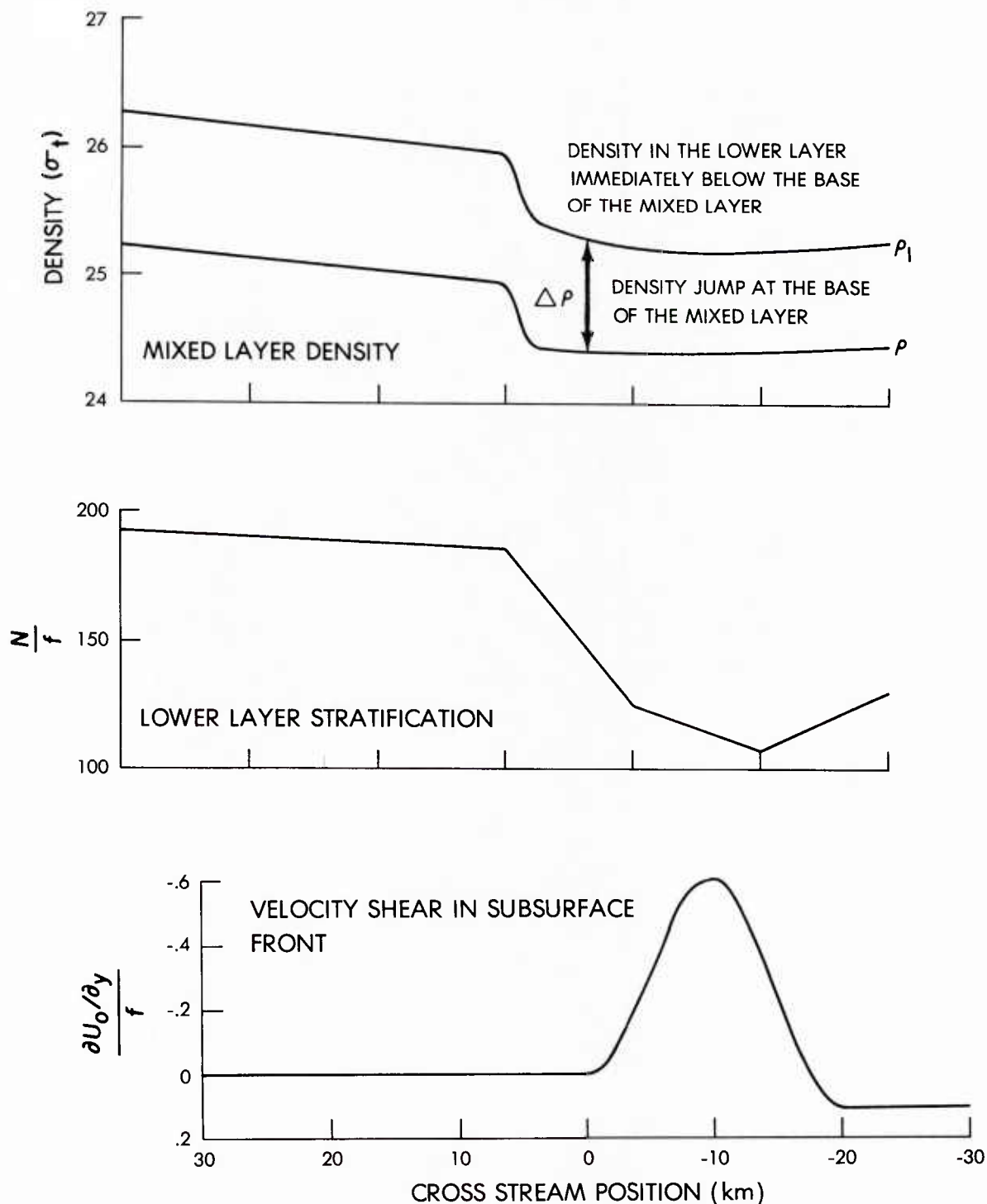


Figure 1. Initial state of the model before the start of the wind stress. After the advent of the wind stress the mixed layer density and the density at the top of the lower layer evolve. The lower layer stratification N and the lower layer cross stream velocity shear $\partial U_0 / \partial y$ remain fixed.

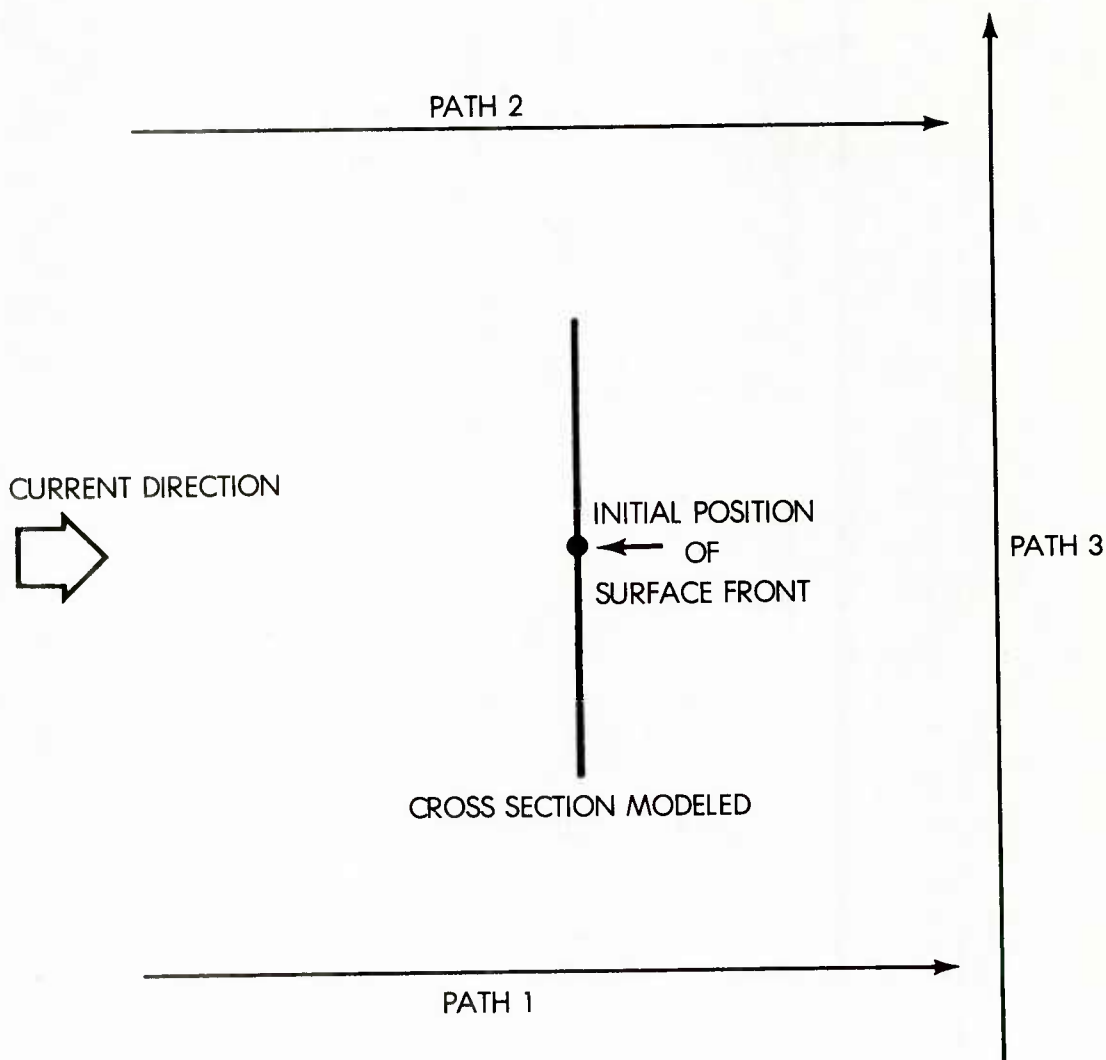


Figure 2. The three storm paths used relative to the cross section of the current modeled. Each of the three paths are straight along which the storm moves with a constant speed of 11 m/s. The first storm path is parallel to the current (eastward) and 44 km to the south of the initial position of the surface front (the position of the subsurface front). The second path is also parallel but is instead 44 km to the north. The third storm path is perpendicular to the current (northward) and 44 km to the east of the cross section modeled.

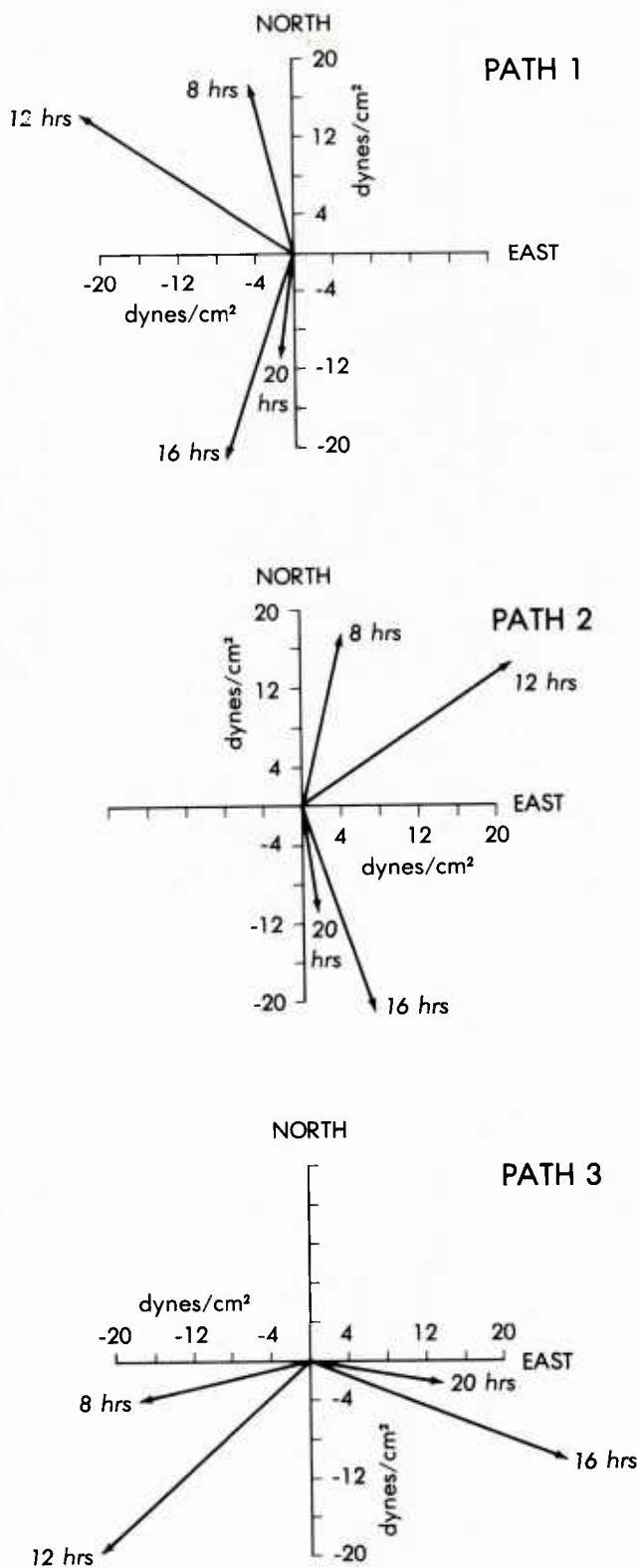


Figure 3. The wind stress vectors versus time obtained using the storm paths described in figure 2 and the hurricane model described in the text. These wind vectors are those at the initial position of the surface front. At any given time the wind vectors vary with cross stream position.

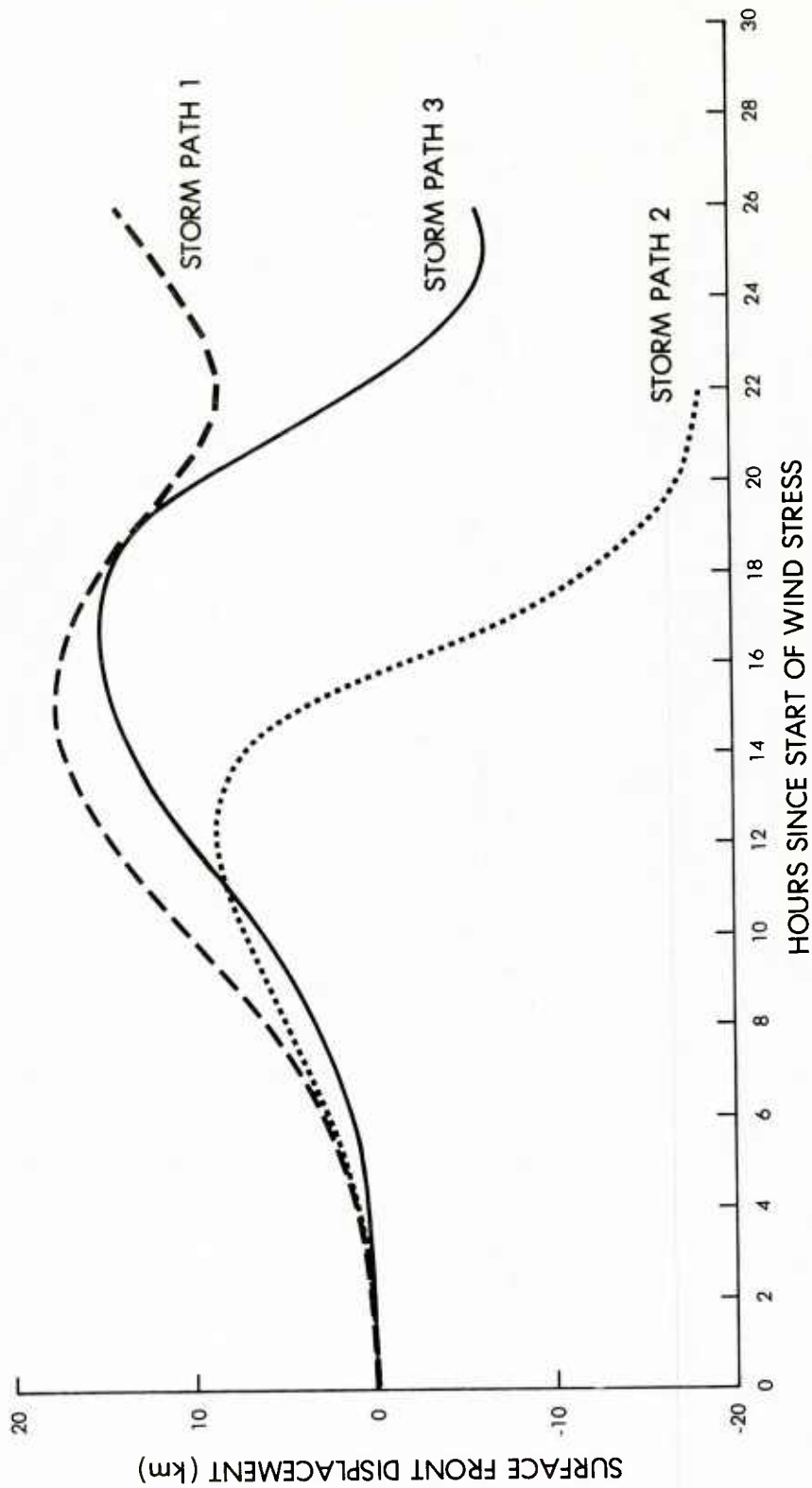


Figure 4. Plots of surface front displacement versus time since start of the wind stress for each of the three storm paths. The wind stresses used are illustrated in figure 2. Positive and negative displacements refer to north and south displacements respectively.

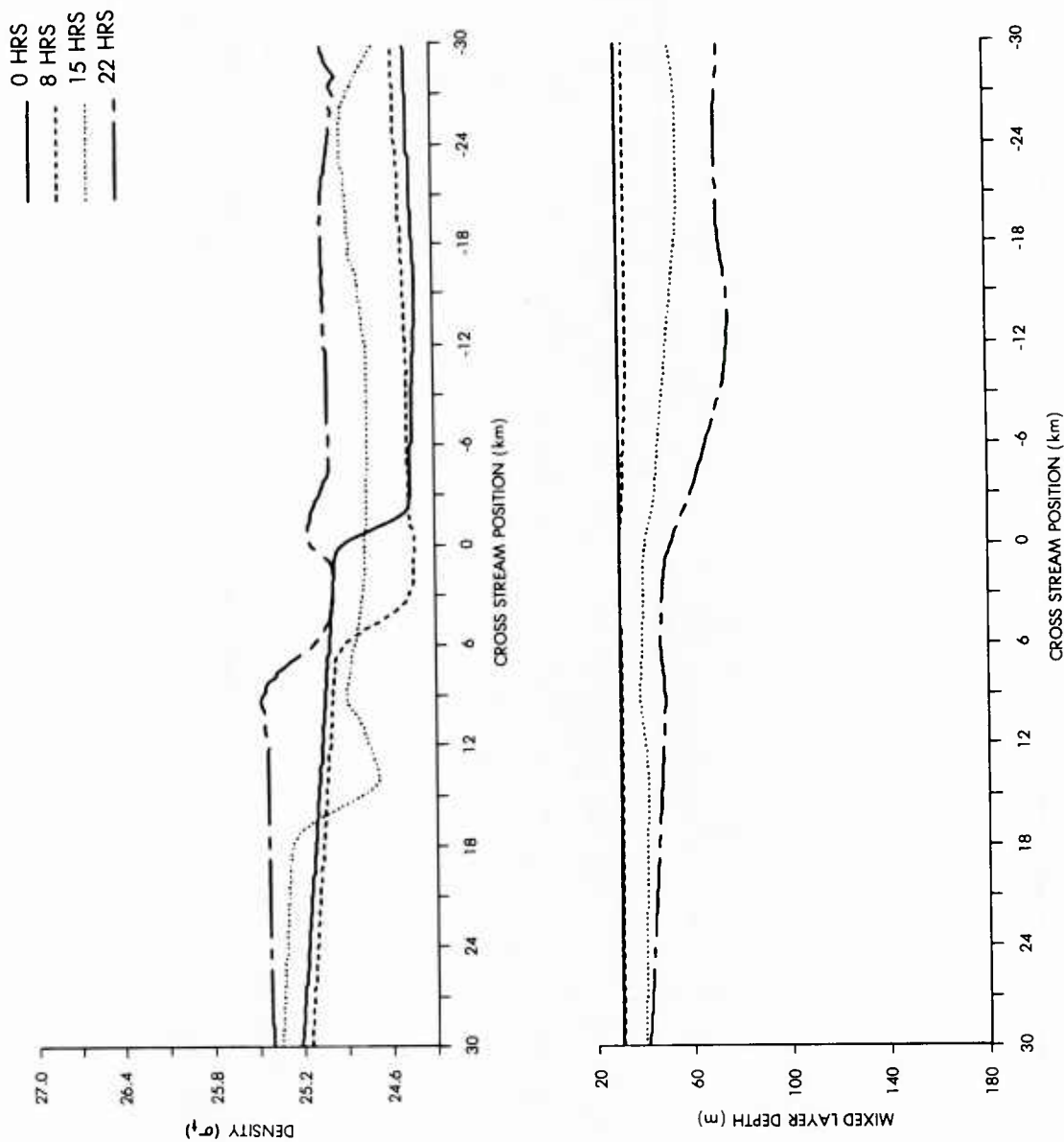


Figure 5a. Mixed layer density and depth changes due to storm path 1. Assumes **confluence** for the continuity balance and momentum balance A.

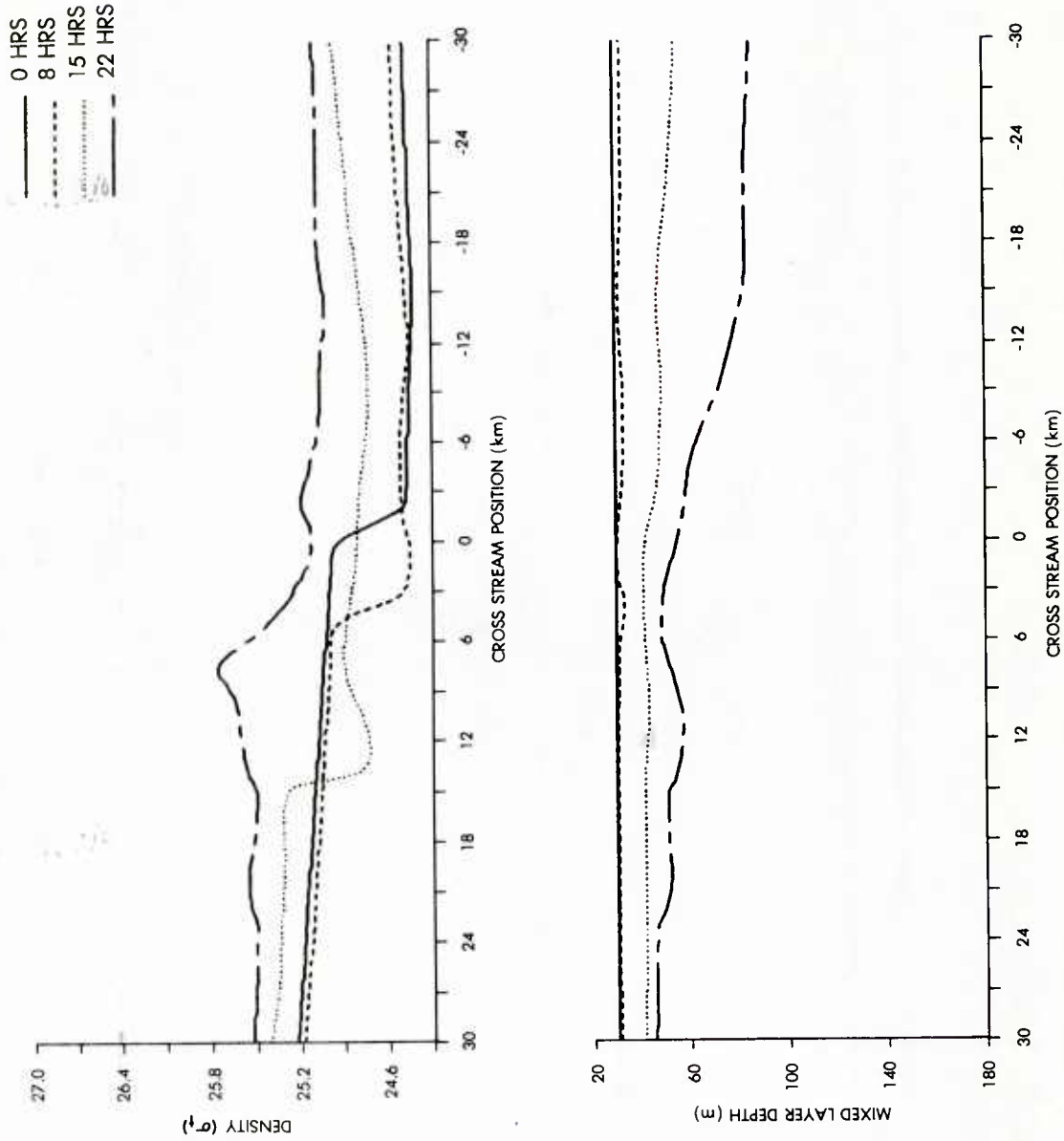


Figure 5b. Mixed layer density and depth changes due to storm path 1. Assumes **confluence** for the continuity balance and momentum balance B. (Same as figure 5a except assumes momentum balance B.)

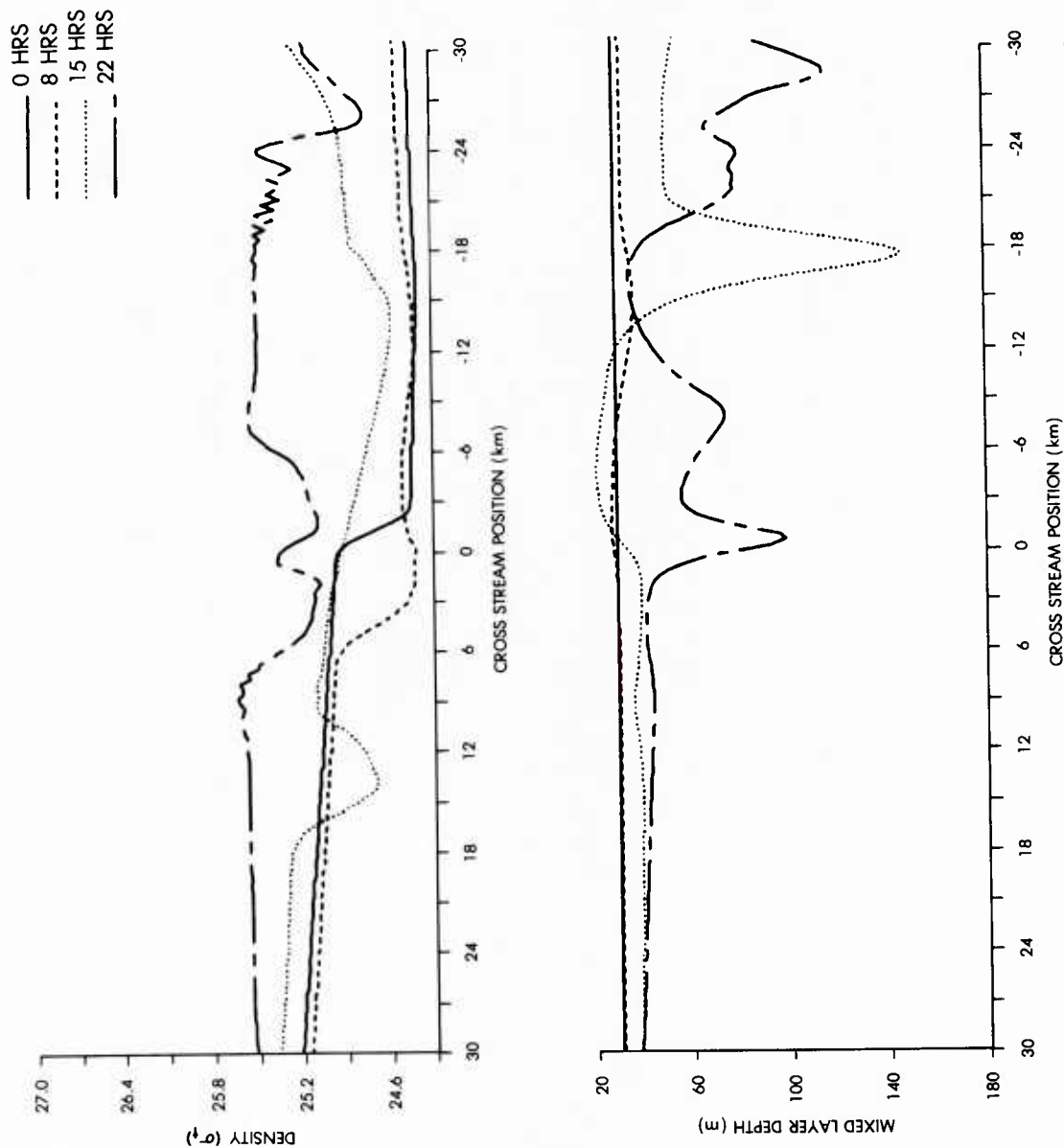


Figure 5c. Mixed layer density and depth changes due to storm path 1. Assumes **convergence** for the continuity balance and momentum balance A. (Same as figure 5a except assumes **convergence** for the continuity balance.)

0 HRS
8 HRS
15 HRS
22 HRS

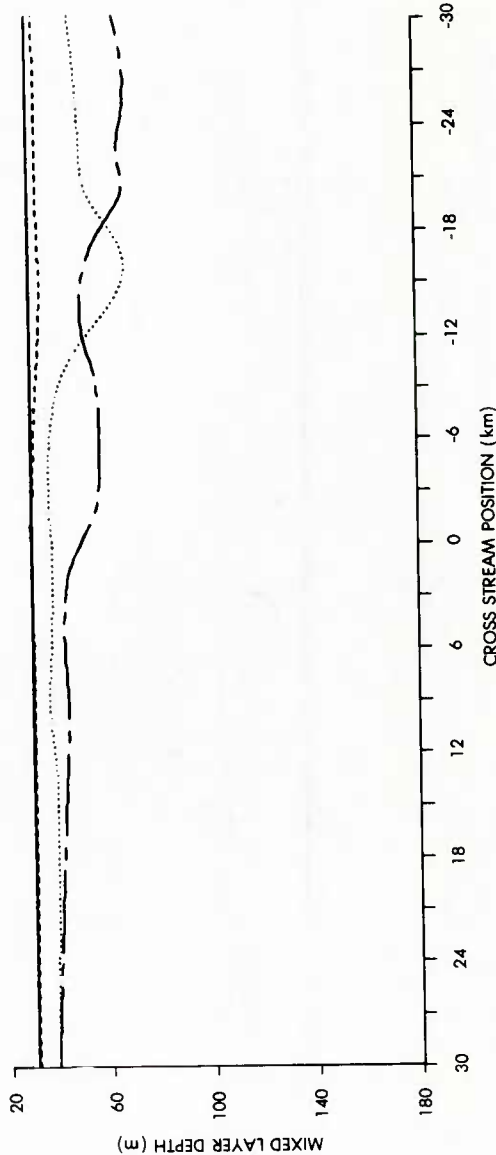
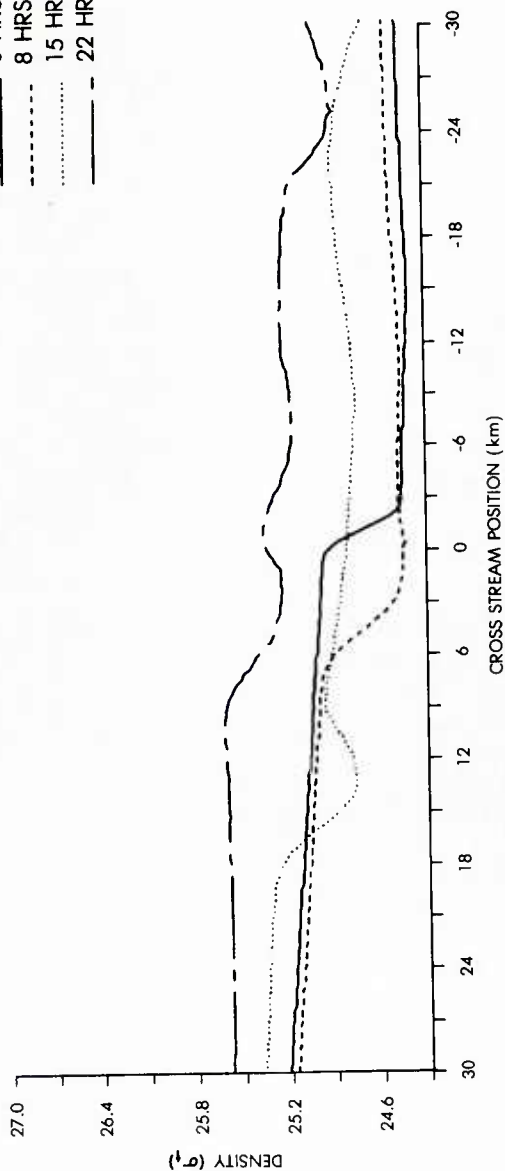


Figure 5d. Same as figure 5c except that the cross stream velocity shear in the subsurface front is much weaker.

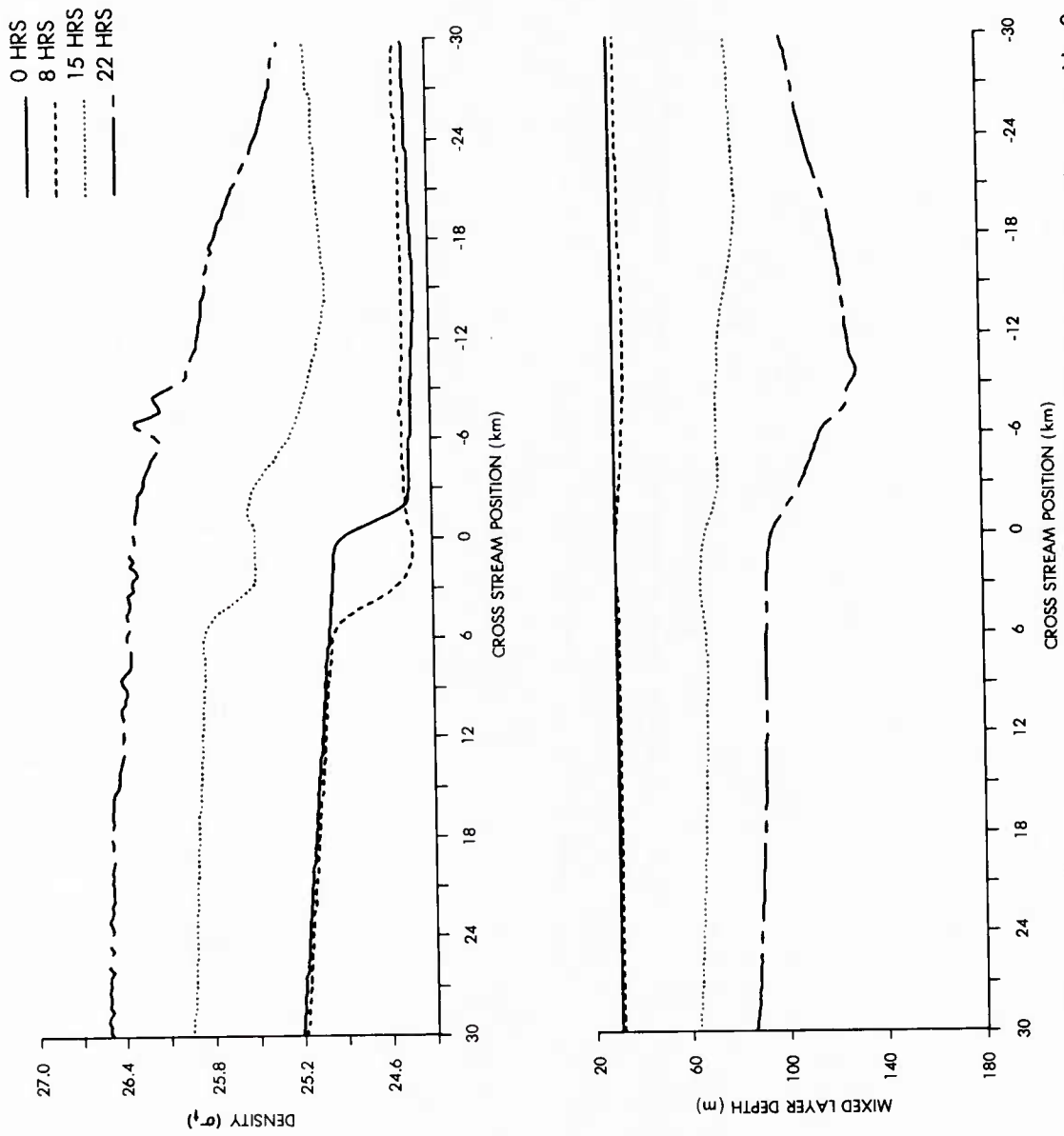


Figure 6a. Mixed layer density and depth changes due to storm path 2. Assumes confluence for the continuity balance and momentum balance A. (Same as figure 5a except uses storm path 2 instead of storm path 1.)

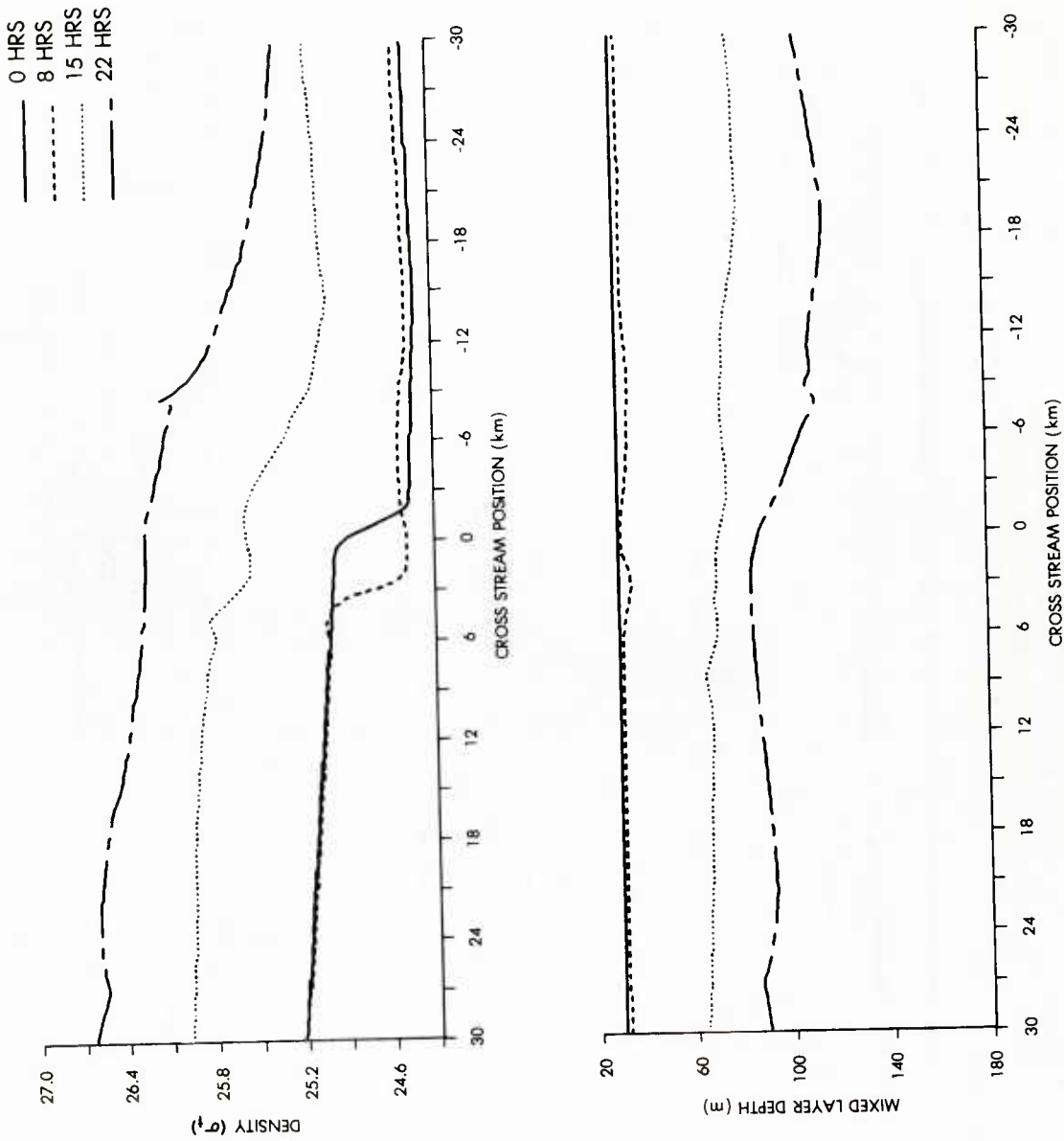


Figure 6b. Mixed layer density and depth changes due to storm path 2. Assumes **confluence** for the continuity balance and momentum balance B. (Same as figure 5b except uses storm path 2 instead of storm path 1.)

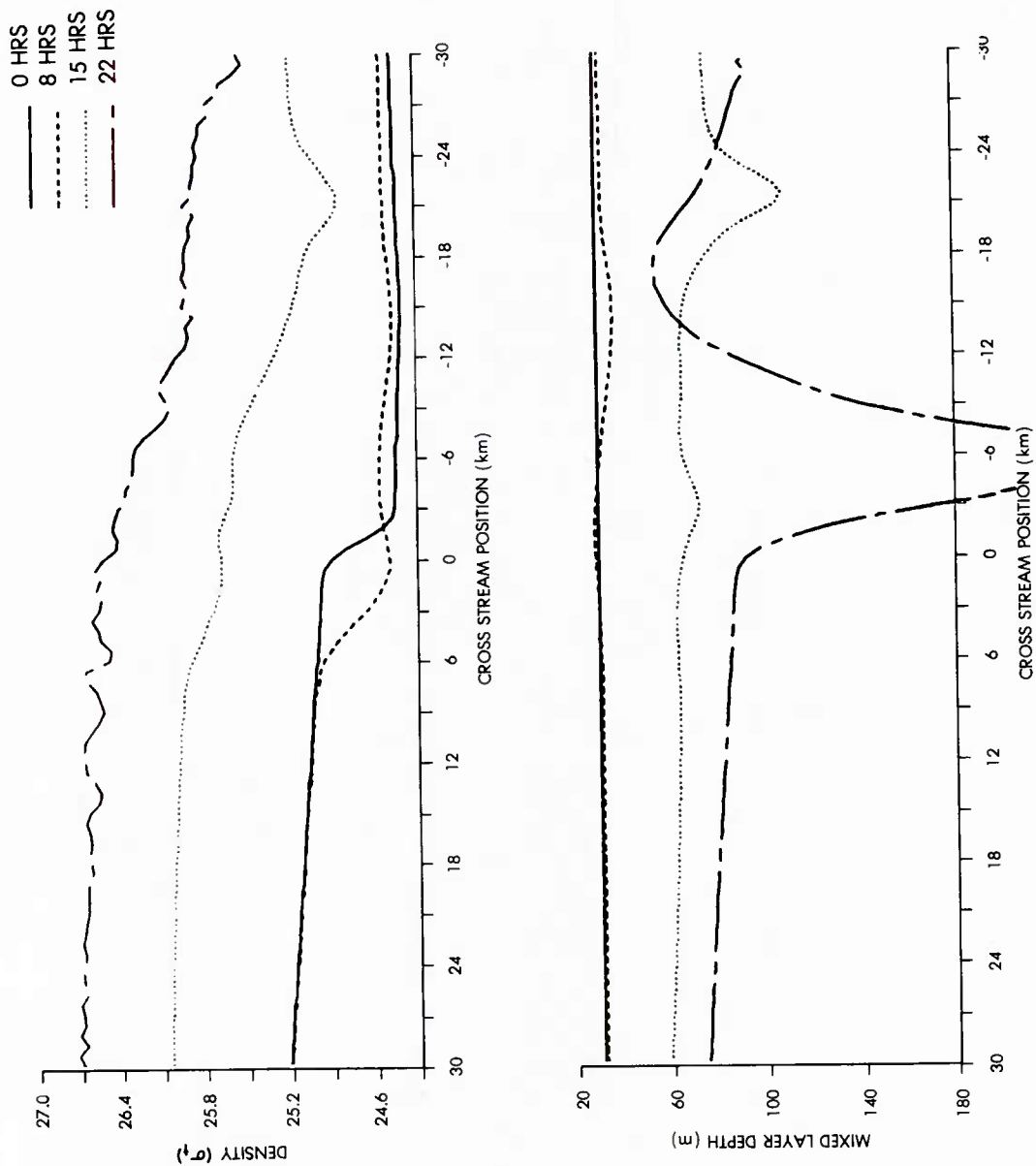


Figure 6c. Mixed layer density and depth changes due to storm path 2. Assumes convergence for the continuity balance and momentum balance A. (Same as figure 5c except uses storm path 2 instead of storm path 1.)

— 0 HRS
 - - 8 HRS
 ··· 15 HRS
 - - 22 HRS

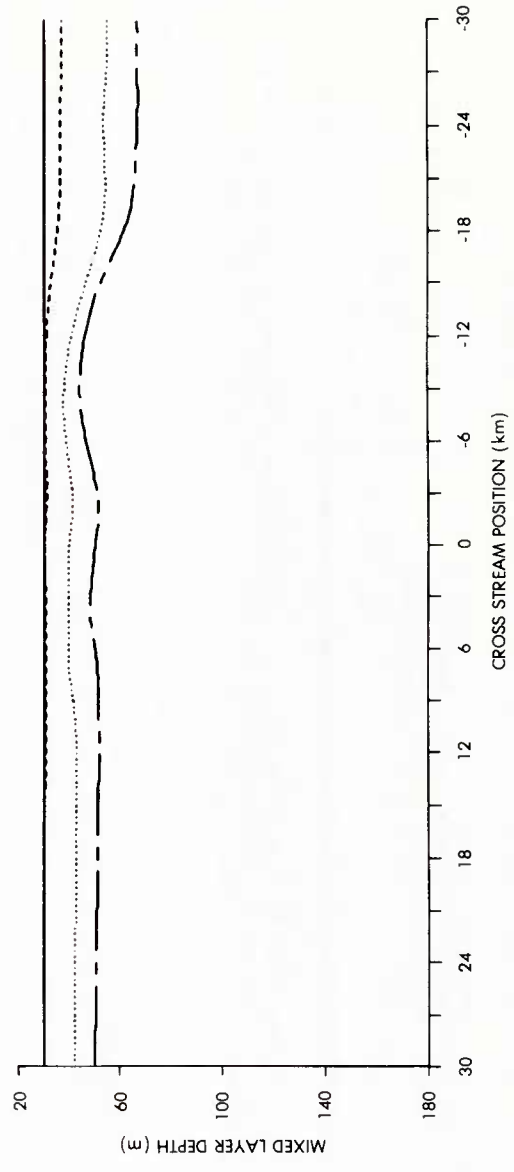
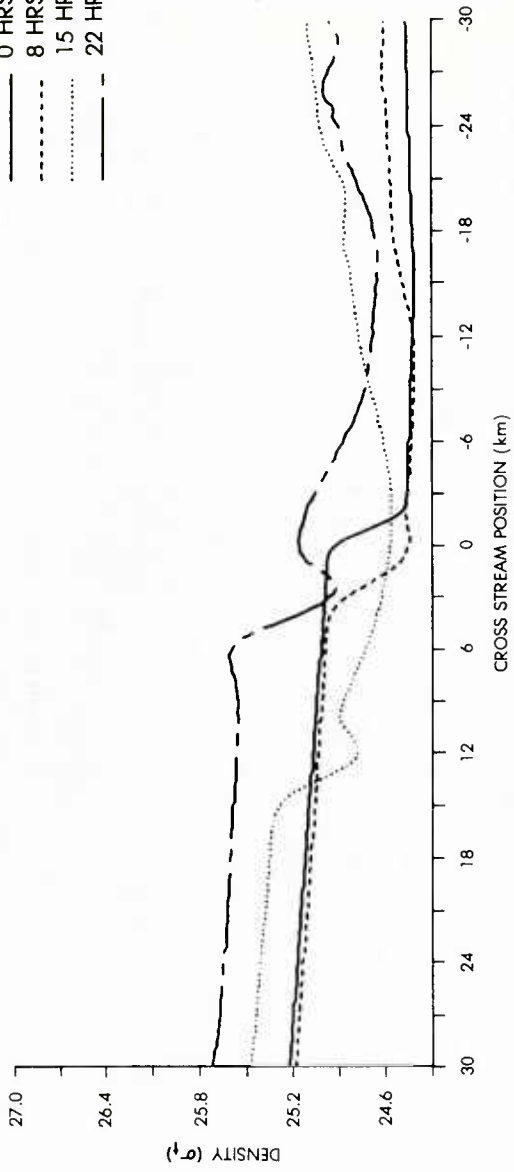


Figure 7a. Mixed layer density and depth changes due to storm path 3. Assumes **confluence** for the continuity balance and momentum balance A. (Same as figure 5a except that storm path 3 is used instead of storm path 1.)

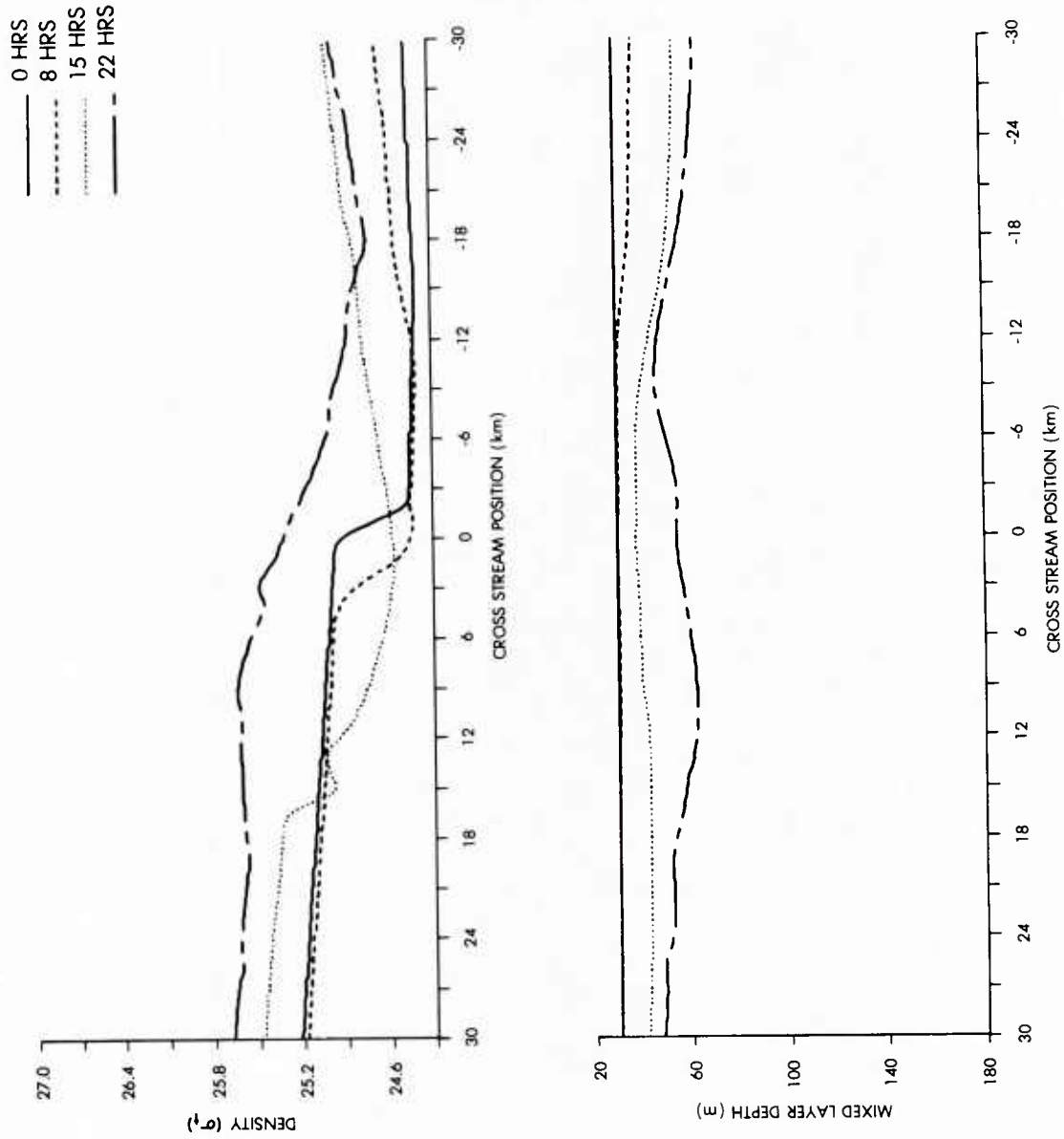


Figure 7b. Mixed layer density and depth changes due to storm path 3. Assumes **confluence** for the continuity balance and momentum balance B. (Same as figure 5b except that storm path 3 is used instead of storm path 1.)

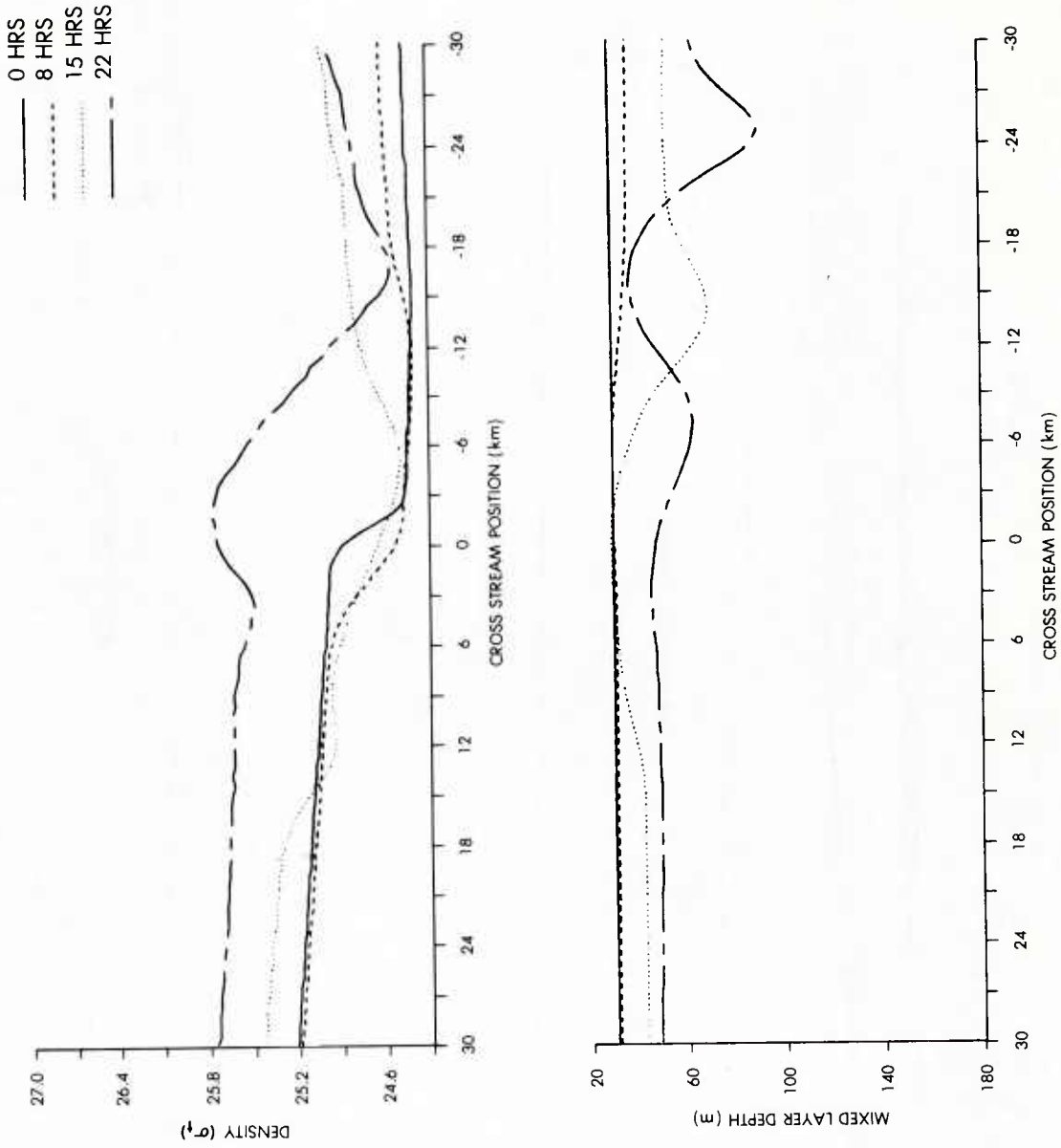


Figure 7c. Mixed layer density and depth changes due to storm path 3. Assumes **convergence** for the continuity balance and momentum balance A. (Same as figure 5c except that storm path 3 is used instead of storm path 1.)

DISTRIBUTION LIST

ALL COMNAVOCEANCOM (COMMAND, CENTERS, FACILITIES, (1 ea)	8
CNO (OP 952, 952D1)	2
CINCLANTFLT (N37C)	1
CINCPACFLT (O2M)	1
COMAREASWFORSIXTHFLT (2D)	1
COMASWINGPAC (N351)	1
COMNAVAIRDEVCEN (203, Library)	2
COMNAVAIRSYSCOM (370P, Library)	2
COMNAVAIRTESTCEN (ASW Directorate)	1
COMNAVSEASYSYSCOM (63D5, Library)	2
COMSUBDEVRON TWELVE (204B)	1
FLENUMOCEANCEN (GTRL)	1
NAVPGSCOL	1
NAVWARCOL	1
NORDA	10
NOSC	1
NRL	1
NUSC (22, 3343, Library)	3

U211786

TECHNICAL REPORT

**GULF STREAM SURFACE
FRONT DISPLACEMENT BY
THE LOCAL WIND STRESS:
A TWO-DIMENSIONAL NUMERICAL
MODEL**

CHARLES W. HORTON

APRIL 1983